Contents lists available at ScienceDirect

Spectrochimica Acta Part B: Atomic Spectroscopy

journal homepage: http://ees.elsevier.com

Assessing the type and quality of high voltage composite outdoor insulators by remote LIBS analysis: A feasibility study

Olga Kokkinaki [a], Argyro Klini [a], Maria Polychronaki [a,b], Nikolaos C. Mavrikakis [c], Kiriakos G. Siderakis [c], Emmanuel Koudoumas [c], Dionisios Pylarinos [d], Emmanuel Thalassinakis [d], Konstantinos Kalpouzos [a], Demetrios Anglos [a,b,*]

[a] Institute of Electronic Structure and Laser, Foundation for Research and Technology-Hellas (IESL-FORTH), P.O. Box 1385, GR 71110 Heraklion, Crete, Greece
[b] Department of Chemistry, University of Crete, P.O. Box 2208, 71003 Heraklion, Crete, Greece
[c] Hellenic Mediterranean University, Department of Electrical and Computer Engineering, P.O. Box 1939, GR 71004 Heraklion, Crete, Greece
[d] Islands Network Operation Department, Hellenic Electricity Distribution Network Operator S.A., ΓΡ 71307 Heraklion, Crete, Greece

ARTICLE INFO

Keywords
HV composite insulators
Laser induced breakdown spectroscopy-LIBS
Remote sensing

ABSTRACT

The use of composite polymeric insulators in overhead high voltage (HV) power transmission lines and in substations has been rapidly growing, as a result of their excellent operational performance, even under environmental pollution conditions. However, it has been observed that the insulation capacity of the composites deteriorates gradually for in-service insulators as a result of ageing, caused by several processes arising because of environmental, electrical and mechanical stresses. For these reasons, development of non-destructive diagnostic techniques for real-time, on-site inspection of the insulators' condition is required for ensuring high reliability of power transmission networks. To this end, laser-induced breakdown spectroscopy (LIBS) is found to offer an effective and reliable method for assessing the state of polymeric insulators, primarily silicone rubber (SIR) ones, that have been in service for up to 20 years on the HV power network of Crete, Greece. Determining the type of composite and furthermore the chemical integrity of the insulator is achieved on the basis of simple spectral indicators, which reflect the extent of chemical modifications induced on the insulator surface. Standard and remote LIBS measurements have been performed in the laboratory. A remote LIBS proof-of-principle diagnostic procedure is presented, which demonstrates that LIBS can become a field deployable technique for the efficient and reliable assessment of the performance of HV outdoor insulators in service. A preliminary test study shows that the remote LIBS approach works reasonably well in the field.

1. Introduction

Composite polymer-based insulators find currently extensive use in high-voltage (HV) power transmission lines replacing the conventional ceramic ones. Combining low weight with high heat resistance, chemical stability and hydrophobicity, these insulators feature excellent long-term behavior, along with reduced installation and maintenance costs. In general, composite polymeric insulators consist of a host polymer matrix containing various inorganic fillers dispersed in it, such as calcium carbonate or alumina, which enhance the thermal, insulating and mechanical properties of the elastomers. The most common polymer composites used in this type of insulators are based on polydimethylsiloxane (PDMS) or ethylene propylene diene monomer (EPDM) as these elastomers have been found to offer enhanced performance even under adverse environmental conditions. In the case of PDMS, commonly known as silicone rubber (SIR), the polymer backbone consists of a cross-linked (-Si-O-) chain network with each Si atom bearing two methyl groups ($-CH_3$), which provide the hydrophobic properties. In contrast, EPDM rubber is a terpolymer system based on the *co*-polymerization of ethylene, propylene with a small amount - on the order of 10% - of a diene, for example, ethylidene norbornene. The polymerization yields a largely poly(ethylene-*co*-propylene) type of backbone with side chains, bearing a carbon-carbon double bond each. These unsaturated moieties produce the required cross-linking.

Despite their favorable properties, SIR and EPDM insulators are subject to ageing via a number of degradation processes, attributed to long-term exposure of the elastomer to varying environmental conditions as well as operation under high electrical stress [1–4]. In addition, deposition of dust and salts, particularly in coastal areas, along with varying levels of moisture, facilitates the formation of conducting films on the insulator surface. These deposits increase the probability of flashover, namely electrical breakdown taking place on the surface

* Corresponding author at: Institute of Electronic Structure and Laser, Foundation for Research and Technology-Hellas (IESL-FORTH), P.O. Box 1385, GR 71110 Heraklion, Crete, Greece.
E-mail address: anglos@iesl.forth.gr (D. Anglos)

https://doi.org/10.1016/j.sab.2020.105768
Received 10 October 2019; Received in revised form 16 January 2020; Accepted 17 January 2020
Available online xxx
0584-8547/

of the insulator [5], thus endangering the integrity of the insulator itself but even more the safety of the whole power network.

Therefore, ensuring that composite insulators perform properly is of high importance and a priority for achieving failure-free operation of the corresponding power transmission network. In this context, extensive studies have been carried out concerning the degradation of field-aged polymeric insulators including chemical analysis by various methods such as Fourier Transform Infrared Spectroscopy (FTIR) [6], X-ray Photoelectron Spectroscopy (XPS) [7], mass spectrometry (MALDI-MS and TOF-MS) [8], Thermogravimetric Analysis (TGA) [9] and Scanning Electron Microscopy (SEM) [10]. All these techniques provide useful results, yet they require removal of the insulators from the transmission lines and sampling of the polymeric housing material before performing measurements. This kind of analytical procedure implies that the insulators examined are, in fact, destroyed and cannot be reinstalled back on the power lines, even if they are found to be not or only minimally aged. Since ageing is strongly linked to environmental conditions, multiple insulators from multiple towers need to be examined, if a reliable estimation is to be achieved concerning the condition of insulators on a particular transmission line or even across a wider area (that may include multiple transmission lines). Such an approach leads not only to a significant increase of maintenance costs but also to disturbance of the power transmission system, hence, alternatives need to be considered.

To this end, the development of suitable diagnostic methods, which would enable remote and real-time evaluation of the insulators condition based on their physical and chemical properties, is essential and could facilitate engineers to make informed decisions as far as maintenance and/or replacement actions are concerned [11]. For assessing the state of in-service insulators, several techniques have been proposed [12], including IR thermography [13], acoustography [14] and optical emission imaging [15]. Although these methods provide useful information concerning the presence of defects, they lack precision, since measurements are compromised by environmental conditions, resulting in rather low values of signal-to-noise ratio (S/N).

Alternatively, spectrochemical methods such as laser-induced fluorescence (LIF) or Raman spectroscopy have been tested as regards their potential for the in-situ analysis of polymeric insulators, since both of them are portable, non-invasive and quite sensitive to the chemical composition changes of materials. In particular, LIF spectra from naturally aged, degraded insulators and from pristine ones, demonstrate profound differences, which have been attributed to growth of microorganisms on the surface of the insulators, that were dependent on environmental conditions [16,17]. Raman spectroscopy has also been employed as a probe to investigate the effects of dielectric breakdown phenomena and other electrical discharges on the chemistry of insulator rubber materials [18,19]. However, despite being quite sensitive, both techniques are prone to interferences arising from uncontrollable surface contamination and as such could fail to provide the required analytical data concerning the insulator chemical integrity. Indeed, preliminary studies performed in the context of this research, on outdoor field-aged composite insulators (from the HV network of Crete), indicated that the detected LIF and Raman scattering signals were affected by the insulator surface contamination and roughness, leading to inconsistencies in the spectral features observed (data not shown), hindering proper evaluation of the insulator condition [20].

In an effort to overcome such limitations, a laser ablation-based method was investigated and found to offer a fast means to quantify and characterize degradation of non-ceramic, out-of-service insulators, based on the observation that the etching depth of the housing material increases with the degree of degradation [22]. Other studies have exploited laser ablation etching with the purpose to rank different insulator housing materials as regards their potential resistance to degradation, in the context of examining candidate material formulations prior to more detailed research [23].

Exploiting laser ablation from a different perspective leads to a well-known technique, Laser-Induced Breakdown Spectroscopy (LIBS), which combines laser ablation sampling of materials, plasma formation and optical probing of the plasma emission. This allows fast determination of the elemental composition of the ablated material. Advantages of LIBS include minimal or zero sample preparation, short (nearly instantaneous) measurement time, and compact and easy-to-use equipment of low maintenance cost. Therefore, LIBS has become a promising technique for monitoring in-situ, remotely and on line the elemental content of materials (in the gas, liquid or solid phase) supporting a wide range of industrial, environmental and life science applications [24–29]. In this context, the use of LIBS could facilitate remote and real-time monitoring of the condition of a large number of insulators in service, with no need to have them removed from the power lines. In fact, a mobile LIBS-LIDAR system [30] has already been examined as regards its potential application for the remote detection of NaCl on silicone rubber insulators as well as for the removal of the salt deposits. Recently, researchers reported that LIBS spectral data, in particular the ratio of ion to neutral line intensity for several elements, appear to correlate with the surface hardness of SIR insulators, which in turn is known to increase with ageing [31]. In a similar study it has been suggested that by use of LIBS coupled to chemometrics, SIR insulators can be classified on the basis of their varying degree of filler content, which relates with the insulator resistance to tracking and erosion [32]. These preliminary studies suggest LIBS as a very promising technique for assessing the physical condition of HV outdoor insulators. However, the use of this technology for targeting the evaluation of the quality of HV field-aged outdoor insulators in real-time and at stand-off distances has not been demonstrated so far, to the best of our knowledge.

In the work presented herein, the effectiveness of LIBS as a diagnostic tool for the assessment of the physical state of in-service HV outdoor composite insulators was investigated. Both standard and remote LIBS measurements were conducted in the laboratory while FTIR analysis was employed as a method to validate the LIBS results. Specific spectral indicators were found to correlate well with the extent of chemical modifications on the insulators surface that resulted from their long-time operation in the field. Finally, to test the applicability of the proposed LIBS methodology, the remote LIBS set up was transported at the Hellenic Electricity Distribution Network Operator (HEDNO) outdoor experimental facility (TALOS High Voltage Test Station). The data obtained show that remote LIBS holds potential for offering a sensitive probe capable of assessing in real-time the operational condition of HV composite field-aged insulators.

2. Materials and methods

2.1. HV outdoor composite insulators

Composite insulators [33] generally consist of a load bearing a glass-fiber-reinforced epoxy rod, a surrounding polymeric housing and metal fittings at both ends of the rod (ground and high voltage) for the transmission of the mechanical loads (Fig. 1). The housing material is designed in a shed-like shape in order to increase the creepage distance (shortest distance, along the insulator surface, between the metal ends of an insulator). Also, such a shape facilitates washout of pollutants by rain.

In the context of a broader investigation, several polymer-based field-aged insulators were removed from certain sites of the 150 kV power transmission network of Crete. For the present work, seven field-aged insulators (No 2–8) were examined along with a pristine one (No 1) used as reference. The selection of insulators was based on the pollution mapping of the network as well as on their operation time in the field [34] and specific information is given in Table 1. The chemi-

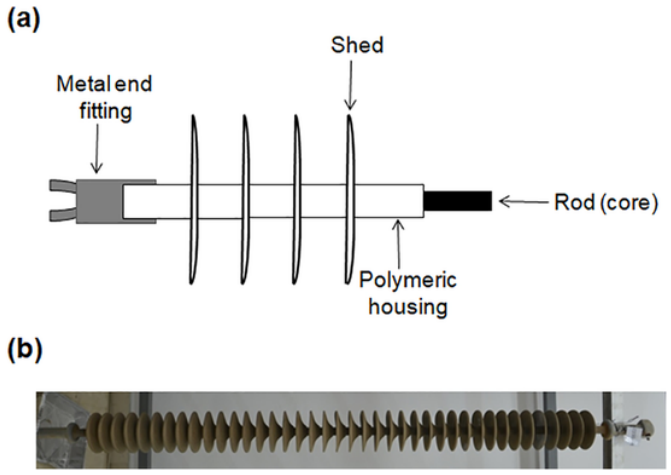

Fig. 1. (a) Schematic representation of the basic components of a HV composite insulator (b) Illustration of a field-aged HV composite insulator, which was detached from the 150 kV transmission network of Crete.

Table 1
Characteristics of HV outdoor composite insulators from the 150 kV transmission network of Crete.

Insulator serial no	Manufacturer	SPS [a]	Operation time (yrs)
1	A	–	0
2	B	Heavy	17
3	B	Light	16
4	C	Heavy	21
5	C	Medium	17
6	C	Heavy	17
7	Unknown	Medium	10
8	Unknown	Heavy	10

[a] Site's Pollution Severity as determined in [34].

cal composition of the insulator polymeric housing material has not been provided by the manufacturing companies.

Concerning the actual analysis, a number of sheds were removed from the insulators, along the polymeric housing. Samples were taken from individual sheds in the form of small pieces, 2×2 cm^2, their thickness ranging from 3 to 5 mm depending on the sampling location on the shed. The elastomer samples were examined by LIBS and FT-IR spectroscopy both on their surface and along the cross section, roughly halfway between the upper and lower side of the shed; this way it was possible to assess compositional differences between the surface and the bulk. For LIBS analysis the samples were used as cut and not subjected to any cleaning. However, prior to ATR-FTIR measurements, the field-aged insulator samples were cleaned with water in an ultrasonic cleaner to remove dust deposited on their surface.

2.2. Experimental set-up and instrumentation

In the present study, the LIBS technique is investigated for its applicability to diagnose the type and quality of HV composite insulators. In a typical LIBS experiment, pulsed laser radiation is focused on the sample and results in plasma formation accompanied by emission, which is characteristic of the chemical composition of the material. Collection of plasma emission may be performed close to the target (standard LIBS) or at a distance from the target (remote LIBS) [35]. In the framework of this work, both standard and remote LIBS measurements were carried out. The field-aged insulators, No 3, 4 and 6, were examined via LIBS and, additionally, by ATR-FTIR spectroscopy in order to formulate a proper diagnostic procedure for the insulators, whereas the rest of them were measured with the purpose to check and validate the suggested procedure.

In the laboratory standard LIBS set up, laser pulses from a Q-switched Nd: YAG laser (Spectron Laser Systems; $\lambda = 1064$ nm; $\tau_{pulse} = 10$ ns) were focused ($f = +75$ mm) on the insulator sample surface resulting in plasma formation. The light emitted by the plasma plume was directly collected by an optical fiber (25 μm in diameter), positioned at a distance of about 1 cm from the irradiated surface, and transmitted into a spectrograph (Mechelle 5000, Andor Technology, spectral resolution $\Delta\lambda = 0.1$ nm) for analysis. The spectrograph was coupled to an intensified CCD detector (ICCD, DH734–Andor Technology) which permitted time-resolved recording of the LIBS spectra, with a short time delay with respect to the arrival of the laser pulse on the sample, thus excluding the strong continuum emission present at the early phase of plasma formation. Laser fluence values (F_{LASER}), employed, were in the range of 10–120 J/cm^2. The laser irradiated area was approximately 3×10^{-4} cm^2.

Test measurements for remote LIBS were performed mainly in the laboratory on intact insulators (approximately 1–1.5 m long) mounted on a specially-designed stage, in such a way that the sheds surface was perpendicular to the direction of the laser beam at approximately 1 m height from floor level. The laser beam from a Q-switched Nd: YAG laser ($\lambda = 1064$ nm; $\tau_{pulse} = 10$ ns; BM Industries, Series 5000) was focused on the insulators' surface by use of a long focal length lens ($f = +5$ m). The emission from the plasma was collected by a Newtonian type telescope (f/4) (Vixen R200SS) located approximately 10 m away from the insulator. The optical fiber was positioned and aligned at the telescope focus ($f = +80$ cm) transmitting light into the spectrometer - ICCD system. The maximum laser fluence employed, in the remote LIBS experiments, was rather low, approximately $F_{LASER} = 10$ J/cm^2, due to the weak focusing of the laser beam at long distance. The irradiated area on the insulators' surface was around 0.02 cm^2.

On-site remote LIBS measurements were performed at the Hellenic Electricity Distribution Network Operator (HEDNO) outdoor experimental facility (TALOS High Voltage Test Station) [36]. The experimental set up was similar to the one used in the laboratory, differing only in the spectrometer used, which was a portable one (Avaspec-2048-2-USB2, Avantes) covering the range of 300–600 nm with spectral resolution approximately at 0.2–0.3 nm and operating at $\tau_D = 1.28$ μs and $\tau_G = 1$ ms.

Acquisition parameters for LIBS measurements, aiming at high values of S/N and S/B (signal-to-background) were optimized by recording spectra at various time intervals after the firing of the laser pulse. In the standard LIBS mode, the delay and integration/gate time were set to $\tau_D = 1.1$ μs and $\tau_G = 10$ μs, respectively whereas in the remote LIBS mode measurements were performed at $\tau_D = 0.6$ μs and $\tau_G = 1$ μs. All LIBS spectra have been corrected on the basis of the spectrometers' grating diffraction efficiency and wavelength sensitivity, with the use of a calibrated light source (Deuterium-Halogen lamp, AvaLight-DH-S, AVANTES).

It is noted that a single LIBS measurement of the housing material on each composite insulator or insulator sample was conducted according to the following sequence: a) the insulator samples were irradiated at 5 different spots with 15 successive laser pulses per spot, producing one spectrum per spot as an average of the last 10 single-laser-shot spectra (the first five pulses of the sequence were used as surface cleaning pulses); b) next the 5 LIBS spectra, obtained at the 5 different spots were averaged resulting in a global average spectrum corresponding to what we defined as one LIBS measurement. This procedure was judged necessary for obtaining reliable LIBS spectra representative of the sample composition.

FTIR absorption measurements were carried out on a Bruker Vertex 70v FT-IR vacuum spectrometer, equipped with a A225/Q Platinum ATR unit with a single reflection diamond crystal, which permits analysis of unevenly shaped solid samples and liquids through total reflection measurements, along a spectral range of 7500–350 cm^{-1}. A KBr beam splitter and a room temperature broad band triglycine sulfate (DTGS) detector were used, while interferograms were collected at 4 cm^{-1} resolution (8 scans), apodized with a Blackman-Harris function, and Fourier transformed with two levels of zero filling in order to yield spectra encoded at 2 cm^{-1} intervals. Before scanning, a diamond crystal background spectrum was recorded and each sample spectrum was obtained by automatic subtraction of the background.

3. Results and discussion

A sequence of experimental campaigns was conducted in order to investigate the feasibility of LIBS as a tool to discriminate among different types of composite insulators and, furthermore, to evaluate the physical condition of an insulator. Measurements were performed initially by use of the laboratory standard LIBS system and once favorable experimental conditions were established and a diagnostic procedure was developed, remote LIBS tests were performed in a laboratory environment and finally outdoors.

3.1. LIBS as a tool for identifying the type of HV composite insulators

At first stage, the possibility to employ LIBS analysis for determining the type of HV insulators was investigated. Measurements were performed both on the surface and the bulk of each insulator sample. Representative LIBS spectra from a pristine (No 1, Fig. 2a) and a field-aged (No 4, Fig. 2b) insulator show emission lines assigned to silicon (Si), carbon (C), magnesium (Mg), aluminium (Al), calcium (Ca), iron (Fe), titanium (Ti), sodium (Na) and hydrogen (H) transitions as well as a distinct molecular emission band arising from CN (Table 2). The CN molecule is formed in the plasma when excited carbon atoms react with nitrogen supplied by the atmospheric air [39–41] and relates strongly to SIR. Likewise, the intense emission form Si relates to the organosilicon elastomer. It is therefore suggested that moderate CN and strong Si emission signals in the LIBS spectra can be considered as offering evidence that the polymer component of the insulator is an organosilicon compound. It is noted that even though carbon is a major constituent of the composite, the spectral line corresponding to C atomic emission (C I: 247.86 nm) appears to be quite weak and this is attributed to the low sensitivity of our detector in the wavelength region below 260 nm. Obviously, a UV-sensitive detector would permit one to use both the C line at 247.86 nm and several Si lines in the range of 243–253 nm.

The rest of the elements, detected, relate to environmental deposits or to the fact that the housing material contains several additives/fillers [37,38], which are mainly inorganic oxides (alumina, silica) or carbonate materials, commonly used to reinforce the insulators' mechanical and electrical properties providing also erosion resistance. For example, strong atomic emission from iron (Fe I: 438.37 nm) is observed in the spectra corresponding to the surface of the field-aged insulator samples, while it is negligible in the bulk (Fig. 2b) and is not observed in the spectra corresponding to the pristine insulator. Considering that the insulators, examined herein, are covered mainly by soil and sand, originating from the coastal line of northern Crete and North Africa respectively, Fe atomic emission features are justified and may serve to detect the presence of surface contamination on field-aged insulators. Sodium has been clearly detected on the surface as well as in the bulk of both new and field-aged insulators samples, based on its distinct atomic emission (doublet yellow line at 588.99, 589.59 nm). Its presence in the bulk (including the pristine insulator), persisting for laser irradiation with several pulses, suggests that Na does not relate to surface contamination, but that a sodium salt, most likely NaCl, has been part of the filler solids. Environmental contamination, due to the proximity of the transmission towers to the coast, could be a plausible scenario but in that case we would expect a much stronger Na emission signal on the outer surface of network insulators.

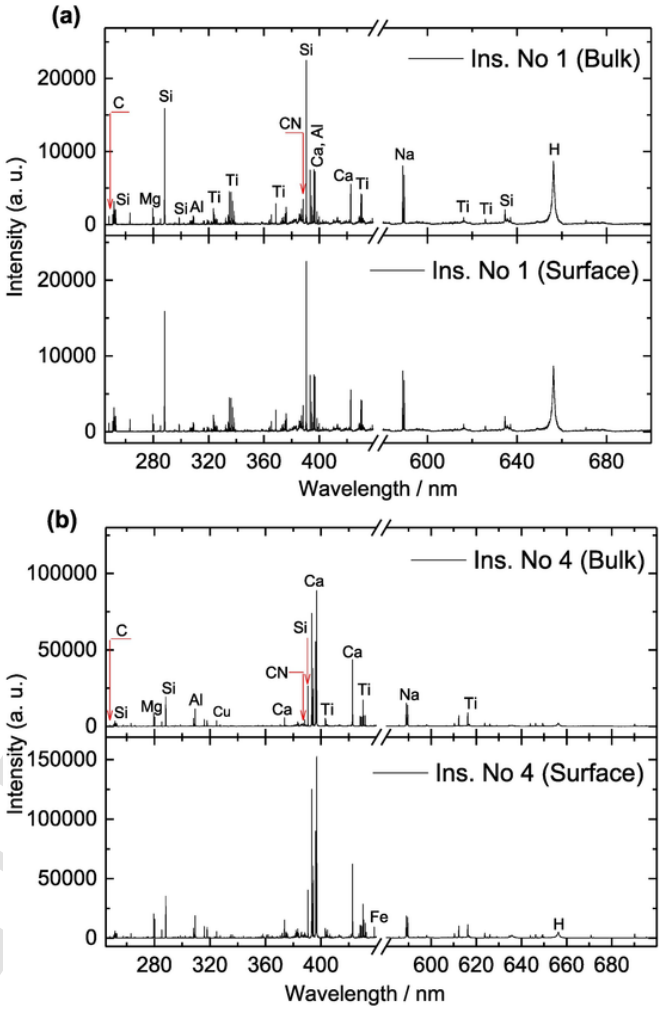

Fig. 2. LIBS spectra recorded in the bulk and on the surface of samples taken from pristine insulator No 1 (a) and field-aged insulator No 4 (b). Each spectrum is an accumulation of 10 single-laser-shot spectra (λ = 1064 nm; F_{LASER} = 120 J/cm^2; τ_D: 1.1 μs, τ_G: 10 μs).

Concentrating our attention to the main components of the elastomer, LIBS spectra from the pristine (No 1) and field-aged insulators (No 4 and 3) are shown in a narrow wavelength range, 387.50–392.00 nm, where emissions related to C and Si are found (Fig. 3). In the case of insulators No 1 and No 4 (Fig. 3a, b) the Si emission line intensity is higher compared to that of the CN emission band head, whereas in the case of insulator No 3, the opposite is observed (Fig. 3c). In order to assess the validity of this observation we need to describe quantitatively these spectral differences and, for this reason, we define the ratio R as:

$$R = I_{CN}/I_{Si} \quad (1)$$

I_{CN} represents the integrated intensity of the CN band head emission (388.34 nm) and I_{Si} the integrated intensity of the Si emission line (390.58 nm). Fig. 4 shows values for R obtained for a series of 10 different LIBS measurements performed, under the same experimental conditions, in the bulk and on the surface of pristine and field-aged insulator samples. The data indicate that R is almost constant in the

Table 2
Main atomic emission lines and molecular emission bands recorded in LIBS spectra of HV outdoor polymeric insulators.

Wavelength (nm) [a]	Assignment
243.51(I), 250.69(I), 251.43(I), 251.64(I), 251.93(I), 252.42(I), 252.87(I), 263.14(I), 288.19(I), 298.77(I), 390.58(I), 634.61(II), 635.53(II)	Si
247.86(I)	C
279.56(II), 280.28(II), 285.25(I)	Mg
308.8(I), 309.28(I), 394.86(I); 394.42(I); 396.15(I)	Al
393.36(II); 396.87(II); 422.69(II)	Ca
431.52(I)	Fe
323.45(II), 323.64(II), 323.9(II), 324.19(II), 326.17(II), 332.32(II), 334.18(I), 334.92(II), 335.49(I), 336.13(II), 337.29(II), 338.41(I), 364.28(I), 365.36(I), 368.54(I), 390.07(I), 395.64(I), 395.85(I), 398.19(I), 429.09(I), 430.11(I), 430.61(I), 453.35(I), 453.56(I), 498.17(I), 499.13(I), 499.98(I), 500.71(I), 501.41(I), 503.64(I), 503.99(I), 506.44(I), 517.38(I), 518.37(I), 519.28(I), 521.01(I)	Ti
588.98(I), 589.6(I)	Na
656.27(I)	H
385.34 (3–3); 386.18 (2–2); 387.13 (1–1); 388.33 (0–0) [b]	CN

[a] Values refer to emission from neutral atoms when followed by (I) and to emission from singly charged positive ions when followed by (II).

[b] Emissions refer to vibronic transitions of CN in the violet system ($B\,^2\Sigma^+ - X\,^2\Sigma^+$) with figures in parenthesis, indicating vibrational quantum numbers for each transition in the upper and lower electronic states.

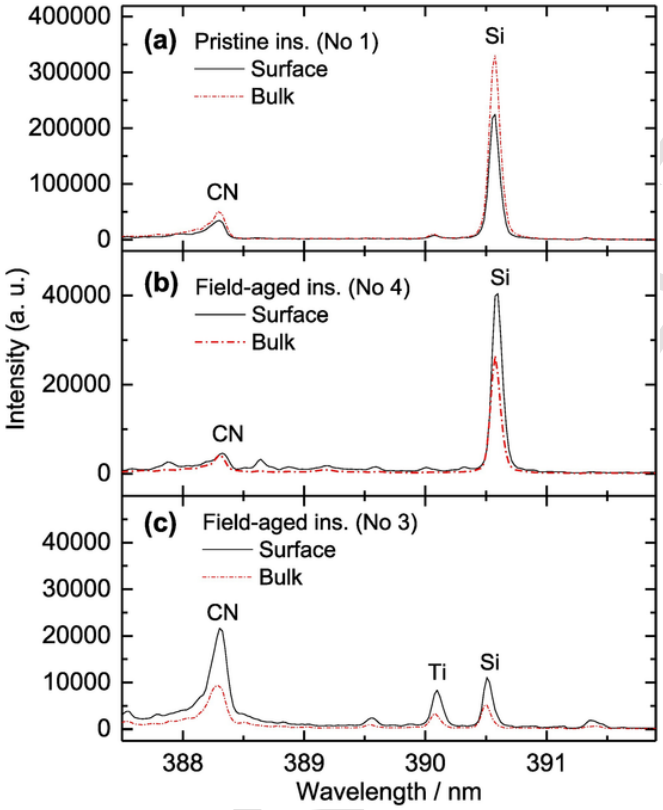

Fig. 3. LIBS spectra recorded in the bulk and on the surface of samples taken from pristine insulator No 1 (a) field-aged insulators No 4 (b) and No 3 (c). Each spectrum is an accumulation of 10 single-laser-shot spectra (λ = 1064 nm; F_{LASER} = 120 J/cm^2; τ_D: 1.1 μs, τ_G: 10 μs).

bulk as well as on the surface of the pristine insulator, providing a reference value, R_{Ref} = 0.31 ± 0.01 (as the average of the individual R values for each one of the 10 measurements) (Fig. 4a). Interestingly, R values calculated from the spectra corresponding to the bulk and to the surface of the two field-aged insulators are either lower, in the case of insulator No 4 (Fig. 4b), or much higher, in the case of insulator No 3 (by almost a factor of 10) (Fig. 4c) compared to R_{Ref}, and this suggests the presence of two types of insulators, which differ in their chemical composition with respect to the pristine insulator.

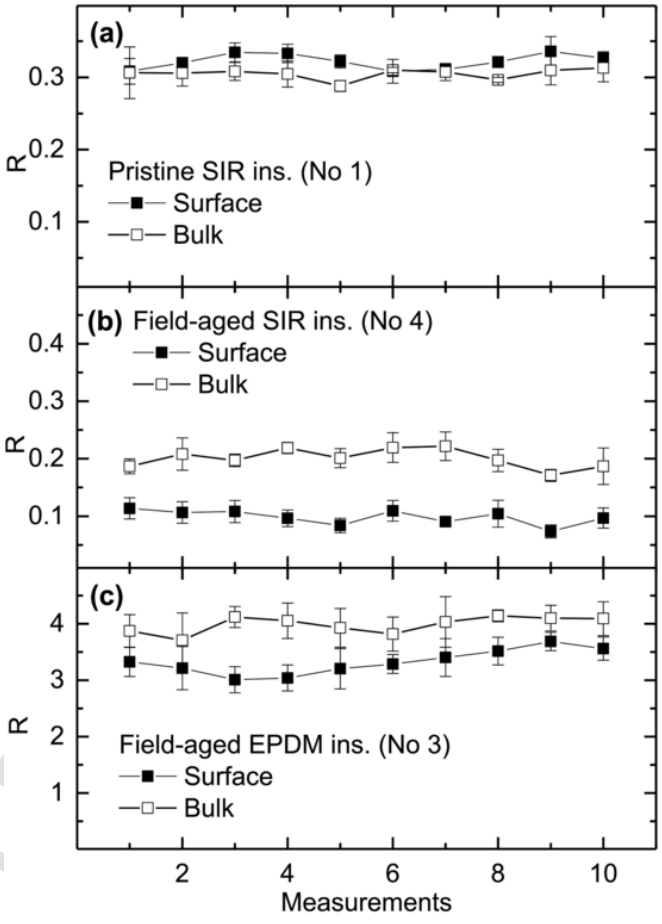

Fig. 4. Mean values of spectral indicator R (Eq. (1)) plotted for 10 separate standard LIBS measurements performed in the bulk and on the surface of samples taken from pristine insulator No 1 (a) and field-aged insulators No 4 (b) and No 3 (c). Each measurement corresponds to irradiation at 5 different spots. The error bars shown for each data point represent standard deviation of the mean value in a set of five R values (λ = 1064 nm; F_{LASER} = 120 J/cm^2; τ_D: 1.1 μs, τ_G: 10 μs).

Indeed, these findings are verified by independent analysis of the examined insulator samples by ATR-FTIR spectroscopy. ATR-FTIR spectra recorded in the range of 4000–600 cm^{-1}, corresponding to the surface and the bulk of pristine (No 1) and field-aged (No 4 and 3) insulator samples are shown in Fig. 5. A reference ATR-FTIR spectrum of pure PDMS is also given for comparison. The spectra obtained from the pristine insulator sample (Fig. 5a) present bands characteristic of SIR [42–45], also observed in the spectrum collected from neat PDMS (Table 3). The same bands are also observed in the spectra corresponding to the field-aged insulator No 4 (Fig. 5b), suggesting that this one is also a SIR insulator. On the contrary, the ATR-FTIR spectra, corresponding to field-aged insulator No 3, are distinctly different, with vibrational bands related to EPDM according to literature data (Table 3) [44,46,47]. Hence, the housing material, corresponding to this field-aged insulator is identified as containing EPDM polymer and not PDMS.

Distinct bands observed in the 3700–3300 cm^{-1} region of the spectra (Fig. 5b, c), corresponding to field-aged insulators No 3 and 4, are assigned to the OH stretching vibrations in alumina trihydrate (ATH - $Al_2O_3{\cdot}3H_2O$) [42,48]. These bands are not observed in the spectrum, recorded from the pristine SIR insulator; instead, a very weak broad band centered around 3410 cm^{-1} is observed (not discernible in

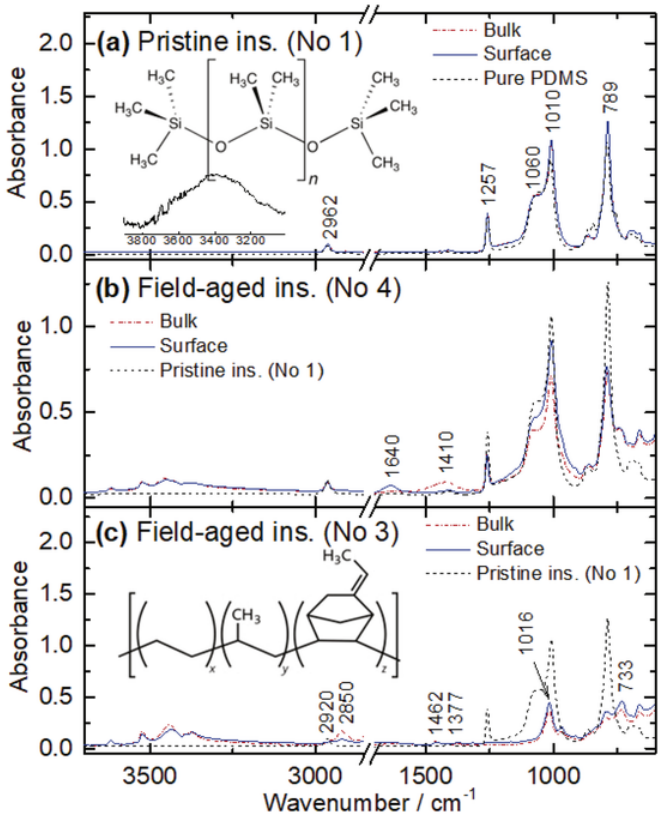

Fig. 5. ATR-FTIR spectra recorded in the bulk and on the surface of pristine insulator (No 1) and pure PDMS (a), field-aged insulator No 4 (b) and field-aged insulator No 3 (c). A reference ATR-FTIR spectrum, recorded in the bulk of pristine insulator is presented for comparison in b and c. The chemical structure of PDMS and EPDM polymers is illustrated in (a) and (c) insets, respectively.

Fig. 5a) and this is assigned to vibrations of water adsorbed on alpha-alumina (a-Al_2O_3) [49,50] (see Table 3). The bands at 1016, 916 cm^{-1}, observed in the EPDM insulator spectrum, are assigned to Al—O symmetric and asymmetric stretching, respectively, in ATH [51,52]. Furthermore, the band at 468 cm^{-1}, observed in the spectra of insulators No 1 and 4, is assigned to Si—O rocking vibrations, whereas the band at 793 cm^{-1}, in the spectrum of insulator No 3, is assigned to Si—O bending [53–56]. These latter bands together with the one at 1069 cm^{-1} (not discernible in our spectra due to overlap with the PDMS bands) are characteristic vibrational bands of silica (SiO_2). Thus, based on the above in combination with the data obtained by LIBS, it is concluded that all the examined insulators contain silica and ATH, except for the reference SIR insulator, which most likely contains anhydrous alumina. Obviously, alumina and silica vibrations are not observed in the spectrum of pure PDMS.

In all, the ATR-FTIR spectroscopic analysis confirms that insulators No 1, 3 and 4 are based on two different types of housing materials. These results correlate well with the LIBS data which give rise to significantly higher R values in the case of the EPDM insulator (No 3), in comparison with the SIR insulators. This is interpreted based on the fact that EPDM contains no Si in its polymer chain. The non-zero value of I_{Si} for insulator No 3 (Fig. 3c) is attributed to the presence of silica (SiO_2) [57,58].

The results obtained by LIBS indicate that the proposed ratio (R) may serve as a *spectral indicator* to discriminate among different types of insulators. We suggest that the comparative LIBS analysis between a field-aged composite insulator of unknown type/structure and a pristine (reference) SIR insulator leads to a sorting criterion (C1) as follows:

Table 3
Main vibrational bands detected in the ATR-FTIR spectra of HV outdoor polymeric insulators.

Wavenumber (cm^{-1})	Ins. no 1	Ins. no 3	Ins. no 4	Pure PDMS	Assignment	References
3695–3375		x	x		-OH stretching in ATH filler	[42,48]
3410	x				-OH stretching in α-Al_2O_3 filler	[48,49,50]
2962	x		x	x	-CH asymmetric stretching in CH_3	[42–45]
2920		x			-CH_2 asymmetric stretching	[44,46,47]
2906	x		x	x	-CH symmetric stretching in CH_3	[42–45]
2851		x			-(CH_2)- symmetric stretching	[44,46,47]
1635–1650		x			-OH in H_2O	[42]
1462		x			-CH_3 asymmetric bending and CH_2 scissoring of CH_3	[42–45]
1445	x		x	x	-CH_3 asymmetric deformation in Si-CH_3	[42–45]
1412	x		x	x	-CH_3 asymmetric bending in Si-CH_3	[42–45]
1377		x			-CH_3 sym. bending and C—H stretching of CH_3	[42–45]
1258	x		x	x	-CH_3 symmetric bending	[42–45]
1060–1010	x		x	x	Si-O-Si asymmetric & *sym*metric stretching	[42–45]
1016		x			-OH bending in ATH filler and Si—O stretching	[51,52]
968		x			-CH bending (out of plane) in CH_3	[47]
916		x	x		-OH bending in Al-OH	[51,52]
864	x		x	x	-CH_3 symmetric rocking in $Si(CH_3)_3$	[42]
843				x	-$Si(CH_3)_2$ vibration	[42]
793		x			-Si-O bending	[52–56]
788	x		x	x	-Si-CH_3 asymmetric rocking & Si-CH_3 asymmetric stretching in $Si(CH_3)_2$	[42–45]
733		x			-(CH_2)- rocking and $(CH_3)_2$ vibration	[44,46,47]
700	x		x	x	-$Si(CH_3)_3$ vibration	[42]
687	x		x		-Si-CH_3 symmetric rocking	[42]
468	x		x		Si-O rocking in SiO_2	[49]

- $R < R_{Ref}$: SIR insulator
- $R > > R_{Ref}$: not SIR insulator

where R and R_{Ref} are the spectral indicator values for the unknown field-aged insulator and the pristine SIR insulator, respectively. The sorting criterion (C1) is fulfilled when $R < R_{Ref}$, which is indicative of the SIR type of the insulator. In cases that this condition is not fulfilled ($R > > R_{Ref}$), the insulator is not classified as a SIR insulator.

3.2. LIBS as a tool for assessing the physical condition of SIR insulators

Further to using LIBS spectral indicators for discriminating among different types of insulators it is even more important to obtain a reliable criterion that will enable assessment of the operational condition of insulators on the field. As mentioned in the introduction, ageing of a composite insulator leads to considerable loss of its surface hydrophobicity and increases the risk of insulator failure. Considering the SIR type of insulators, it is known [59,60] that the reduction of hydrophobicity relates to processes, which involve the removal of methyl groups from the PDMS chains and their replacement with hydroxyl groups, which are responsible for the increase of surface polarity. It has been found that this change in chemistry is predominant on the surface of the insulators rather than in the bulk. On the basis of this fact, we examined the LIBS spectral indicator R (see Eq. (1) considering that its value, in the bulk (R_B) and on the surface (R_S) of an insulator, might reflect the relative amount of carbon over silicon atoms in the polymer, thus serving as an indirect measure of any possible loss of methyl groups. As already shown in Section 3.1, the value of R obtained in the case of the pristine SIR insulator remains effectively constant in the bulk and on the surface, namely $R_B \approx R_S$, with an average value of 0.31 ± 0.01. We consider this value representative of a high quality SIR insulator and use it as a reference, R_{Ref}, against which we compare R_B and R_S values measured for field-aged SIR insulators. In that case, any possible deviations of R_S and/or R_B from the reference value would indicate modifications in the chemical composition of the insulator housing material as a result of ageing. It is noted that no spectral indicators of the physical condition of EPDM insulators are calculated, since, in this case, R has no physical meaning (it does not reflect C/Si chemical composition changes occurring within the polymer chain).

Indeed, in the case of field-aged SIR insulators, the values of R, measured on the surface, are lower than the ones measured in the bulk and both of them are lower in comparison to the reference value, namely $R_S < R_B < R_{Ref}$ (see Fig. 4 and Table 4). This result implies that the field-aged SIR insulators have suffered chemical degradation, not only on the surface, but also, in the bulk and it is consistent with ATR-FTIR measurements. Noticeable reduction of the absorbance at 2962, 1446–1413, 1257 and 789 cm^{-1} was observed in the spectra (Fig. 5b) corresponding to the surface over those collected from the bulk of field-aged SIR insulators. This reduction in absorbance may be attributed to fragmentation of Si-CH_3 bonds in the PDMS backbone. In addition, the absorbance at 1010 cm^{-1} was found to increase on the surface, contrary to that at 1060 cm^{-1}, which was slightly reduced, indicating formation of Si-alkyl and/or Si—O groups and scission of Si-O-Si bond, respectively. Degradation of field-aged SIR insulators is also evidenced by an increase in the absorbance on the surface at 1640 cm^{-1}, which is attributed to water, and an absorbance decrease in the 3600–3200 cm^{-1} region, corresponding to ATH, observed on the surface, in comparison to the bulk. The appearance of new bands, assigned to OH and Si-OH groups, is attributed to migration of low molecular weight polymeric species from the bulk to the surface [61].

Quantification of the SIR degradation, based on the ATR-FTIR analysis, may be possible by calculating AR (absorbance ratio), a spectral indicator reflecting the ratio of the integrated area of spectral bands corresponding to Si-O-Si and Si-CH_3 vibrations at 1060–1010 cm^{-1} and 1258 cm^{-1}, respectively [52,62,63]. The value of AR was found to be the same in the bulk and on the surface of the reference SIR insulator but increased in the case of field-aged SIR insulators surface values exceeding those measured for the bulk (see Table 5) in agreement with a previous study reporting increasing values of AR as indicative of higher degree of SIR degradation [63].

On the basis of LIBS results, the deviation of R values in the bulk or on the surface (R_B or R_S) of field-aged SIR insulators relative to R_{Ref} may be expressed as:

$$\%\Delta R = 100\ \left(1 - R/R_{Ref}\right)\% \quad (2)$$

Therefore, the values of $\%\Delta R_B$ and $\%\Delta R_S$ can be interpreted as reflecting the extent of chemical degradation and, thus, the degree of ageing of the field-aged SIR insulator. Henceforth, %ΔR will be referred to as the LIBS spectral indicator of the physical condition of field-aged SIR insulators.

The spectral indicators R and ΔR calculated from LIBS data obtained in the bulk and on the surface of all tested SIR insulator samples as well as the wettability class determined for each insulator are presented in Table 4. The wettability classification measurements were performed according to the IEC/TS 62073 standard [64] by implementing spray test and contact angle measurements prior to contamination removal. The insulator surfaces are classified according to wettability class (WC) values ranging from 1 to 6, the highest corresponding to a hydrophilic surface [65]. The reference insulator and the field-aged insulator No 8 are characterized as having hydrophobic surfaces, whereas the field-aged insulators No 4 and 6 were found to be partly wettable. We have chosen the %ΔR value of approximately 30% to indicate a transition value, above which an insulator surface is considered semi-wettable and not hydrophobic.

On the basis of the good reproducibility of the calculated spectral indicators, and taking into account the wettabilty classification of the insulators, the following evaluation criterion (C2) for field-aged SIR insulators is proposed:

- % ΔR < 30%: the physical condition of a SIR field-aged insulator is good

Table 4
Spectral Indicators for HV outdoor SIR insulator samples obtained by the standard LIBS method.

Insulators no	Operation time (yrs)	R_S	R_B	R_{Ref}	ΔR_S [a] (%)	ΔR_B [b] (%)	WC [c]
1	0	0.32 ± 0.01	0.30 ± 0.01	0.31 ± 0.01	–	–	1
4	21	0.10 ± 0.01	0.20 ± 0.02	"	69 ± 4	36 ± 6	4
6	17	0.08 ± 0.02	0.18 ± 0.01	"	74 ± 7	42 ± 4	3
8	10	0.23 ± 0.02	0.25 ± 0.01	"	20 ± 5	26 ± 7	2

[a] ΔR_S (%) = $100^x(1 - R_S/R_{Ref})$. R_S : spectral indicator from the surface of the field-aged insulators; R_{Ref} : reference spectral indicator, from a pristine SIR insulator.

[b] ΔR_B (%) = $100^x(1 - R_B/R_{Ref})$. R_B : spectral indicators in the bulk of the field-aged; R_{Ref} : reference spectral indicator, from a pristine SIR insulator. The uncertainty in the calculation of R_S and R_B corresponds to the standard deviation in a set of 10 measurements.

[c] Wettabilty Class (WC) determined according to IEC TS 62073 [64]. (1–2: hydrophobic surface, 3–5: semi-wettable surface, 6–7: hydrophilic surface).

Table 5
Absorbance ratio values (AR) in the ATR-FTIR spectra recorded in the bulk and on the surface of field-aged SIR insulators.

Insulator no	Operation time (yrs)	AR [a] (Bulk)	AR [a] (Surface)
1	0	15 ± 1	15 ± 1
4	21	16 ± 1	21 ± 1
6	17	18 ± 1	20 ± 2

[a] $AR = I_{(1060–1010)}/ I_{1258}$. I: integrated intensity of the bands at 1060–1010 cm^{-1} and 1258 cm^{-1} in the ATR-FTIR spectra corresponding to the bulk and to the surface of field-aged SIR insulators. The uncertainty in the calculation corresponds to the standard deviation in a set of 3–5 measurements.

- % ΔR > 30%: the physical condition of a SIR field-aged insulator is poor

Therefore, a field-aged SIR insulator exhibiting %ΔR < 30% is considered to be in a good physical condition (high quality), otherwise it is considered to have undergone minor or major degradation (moderate or low quality, respectively). The higher the %ΔR values obtained, the lower the quality of the insulator tested. Based on this criterion, and taking into account the ΔR values presented in Table 4, we conclude that the field-aged SIR insulator, No 8, is in quite good condition, while, No 4 is of moderate and No 6 of low quality. Both No 4 and No 6 insulators show clearly that their surface has degraded more than the bulk.

3.3. Remote LIBS diagnostic procedure for the type and physical state of HV composite insulators

Next, the capability to perform LIBS analysis of insulators at a distance was investigated. For this reason, the standard LIBS setup was modified to a remote system, and tested, first, in the laboratory and, finally, in the field. Several intact insulators, which had been out of service and detached from the network, were examined, according to a simple remote LIBS procedure as outlined in Section 2.2. The choice of this simplified approach is justified under the scope of this study, which is to demonstrate the proof-of-concept for successful remote diagnosis of the quality of SIR insulators via LIBS, and not the development of the technical instrumentation or the software required to control the process, which is necessary for the implementation of the methodology in real-case situations.

Remote LIBS characterization of intact insulators involves calculation of LIBS spectral indicators only on the surface of field-aged insulators, since measurements in the bulk of in-service insulators are not possible. Spectral data showed the emission from the plasma to be significantly weaker, with an average emission lifetime of 1.5 μs, significantly shorter in comparison with what was measured in the standard LIBS mode (about 6 μs). This was apparently due to the relatively low F_{LASER} values (10 J/cm^2) on the insulator surface resulting from the weak focusing at long distance. Consequently, LIBS spectra in the remote analysis mode were recorded starting at earlier time delay settings and for shorter time intervals (τ_D = 0.6 μs, τ_G = 1 μs) than in the case of standard LIBS mode.

Field-aged SIR insulators were irradiated at several random points (spots) on their surface. Fig. 6 shows typical remote LIBS spectra for the pristine SIR insulator and for the field-aged ones, No 3, 4, 6 and 8, in the 387.5–392.0 nm range. The surface spectral indicator values, R_S, were found to be comparable or much higher (No 3) than the reference spectral indicator value, R_{Ref}. Hence, it appears that the sorting criterion, defined in Section 3.1, remains reliable when data are collected in remote LIBS mode. Therefore, it is concluded that all the examined field-aged insulators contain SIR as housing material, except for insulator No 3, which is made of EPDM polymer. Next, the spectral indicators, ΔR, reflecting the physical condition of field-aged SIR insulators were also calculated and the evaluation criterion defined in Section 3.2 was applied. The results are in good agreement with those obtained with standard LIBS analysis, indicating that insulator No 8, is of high quality, while insulators No 4 and 6 are of low quality (Table 6). Based on the above results, a remote LIBS measurement procedure along with a diagnostic procedure for the assessment of the type and quality of HV polymeric insulators was formulated in a series of steps and the corresponding flow chart is presented in Fig. 7.

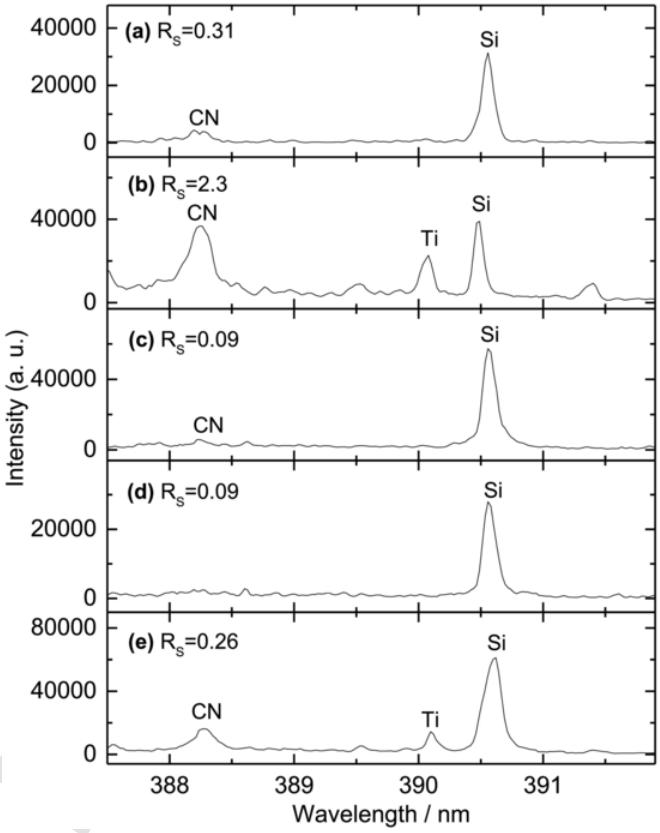

Fig. 6. Remote LIBS spectra of pristine insulator (a) and field-aged insulators No 3 (b), No 4 (c), No 6 (d) and No 8 (e). The calculated surface spectral indicator (R_S) is noted in each case. Each spectrum represents an average of 10 single-laser-shot spectra, recorded upon irradiation of the surface of each insulator on a single spot (λ = 1064 nm; F_{LASER} = 10 J/cm^2; τ_D: 0.6 μs, τ_G: 1 μs).

The first step (Step 1) of the procedure is a critical step, as it concerns targeting the insulator. Targeting ensures that a proper set of areas (spots) on the sheds are examined for obtaining statistically representative results. In real case studies, which require evaluation of in-service insulators, the laser beam should be allowed to scan the insulator's surface either through a telescope, which may be controlled in a way that permits laser beam movement over the shed surface or by guiding the laser beam close to the insulator through a set of optical fibers [24,67]. Other alternatives may exploit drone systems [68].

Step 2 involves irradiation of the selected area (spot) on the field-aged insulator's surface with several successive laser pulses (15 in the present study) and acquisition of the corresponding LIBS spectrum followed by calculation of the spectral indicator, R. This step is repeated for 5 adjacent spots on the surface of the field-aged insulator and an average value for the spectral indicator, R, is obtained. The surface spectral indicator, R_{Ref}, corresponding to a pristine SIR insulator is also measured as reference by following the same procedure.

In Step 3 the insulator type sorting criterion (C1) is applied and, if satisfied ($R < R_{Ref}$), then the insulator is classified as a SIR one. Otherwise, ($R >> R_{Ref}$), another sorting criterion is required, which will al-

Table 6
Spectral indicators for HV outdoor field-aged SIR insulators obtained by the remote-LIBS method.

Insulator no	Operation time (yrs)	R_S	Type [a]	ΔR [b] (%)	Quality [c]	Type [d]	WC [e]
1	0	0.31 ± 0.03	SIR	–	–	SIR	1
3	16	2.22 ± 0.06	Not SIR	–	–	EPDM	
4	21	0.07 ± 0.02	SIR	76 ± 7	Low	SIR	4
6	17	0.11 ± 0.02	SIR	64 ± 7	Low	SIR	3
8	10	0.26 ± 0.02	SIR	18 ± 10	High	SIR	2
Validation							
2	17	2.28 ± 0.09	Not SIR	–	–	EPDM	
5	17	0.10 ± 0.01	SIR	67 ± 4	Low	SIR	3
7	10	0.12 ± 0.01	SIR	62 ± 5	Low	SIR	3

[a] determined by the sorting criterion (C1) (see Section 3.1).
[b] $\Delta R = 100\ (1 - R_S/R_{Ref})$. R_S, R_{Ref} is the average spectral indicator on the surface of field-aged and pristine SIR insulators, respectively ($R_{Ref} = 0.31 \pm 0.03$). The uncertainty in the calculation of average spectral indicators corresponds to the standard deviation in a set of 10 measurements.
[c] determined by use of evaluation criterion (C2) (see Section 3.2).
[d] based on ATR-FTIR measurements.
[e] Wettability Class (WC) determined according to IEC TS 62073 [64]. (1–2: hydrophobic surface, 3–5: semi-wettable surface, 6–7: hydrophilic surface).

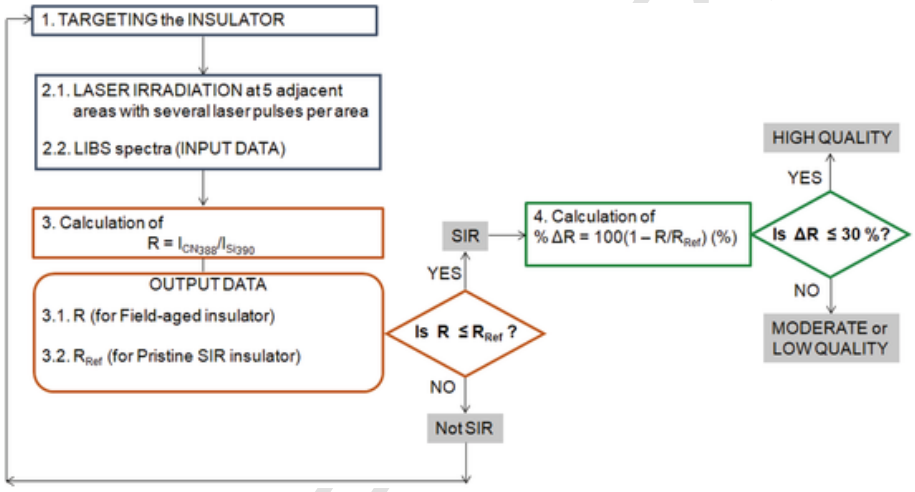

Fig. 7. Flow chart describing the proposed remote LIBS diagnostic procedure for assessing the type and physical condition of HV field-aged SIR insulators.

low classification of other types of polymeric insulators. This is actually one of our goals in future studies. However, in the present work, steps 1 to 2 are repeated, until criterion C1 is satisfied and a SIR insulator is found, so that we proceed to the next step, which involves only SIR insulators.

In Step 4, calculation of ΔR (see Eq. (2) is performed and the evaluation criterion C2 is applied: In the case of $\Delta R < 30\%$, the quality of the examined SIR insulator is considered as high. Otherwise, the insulator quality is moderate or poor. The more ΔR approaches the 100% value, the higher the deviation of the field-aged insulator's quality from the high quality, which corresponds to the pristine insulator of no operation time in the field.

With the above stepwise procedure in place, three field-aged insulators, No 2, 5 and 7, of unknown type and quality, which were also removed from the power transmission network of Crete, were examined as a test of the suggested diagnostic procedure. Typical LIBS spectra, obtained on a single irradiated spot, are presented in Fig. 8 along with the corresponding values of the surface spectral indicators (R_S). Average spectral indicators, derived from spectra corresponding to 10 measurements originating from 10 different spots, are presented in Table 6. The surface spectral indicator value, corresponding to insulator No 2, was found to be significantly higher (approximately by a factor of 7) than the reference SIR spectral indicator value R_{Ref}, therefore it was not registered as a SIR insulator, according to sorting criterion C1. Moreover, the spectral indicator values (see Eq. (1) corresponding to insulators No 5 and 7, were found to be lower than the reference value, both yielding ΔR in the range of 60–70% (see Eq. (2), implying that these insulators are SIR ones of low quality. The mean R and ΔR values are presented in Table 6.

The result of the remote LIBS diagnostic test, as regards the type of the examined insulators, was confirmed by ATR-FTIR spectroscopic analysis. Indeed, Fig. 9 shows ATR-FTIR spectra in the range of 1350–700 cm^{-1} which present bands characteristic of SIR for field-aged insulators No 5 and 7. Insulator No 2 had a distinctly different FTIR spectrum (not shown here) that was similar to the one obtained from insulator No 3 (Fig. 5c), confirming that the polymer matrix was composed of EPDM. From a quantitative standpoint, the ATR-FTIR absorption bands ratio (AR), corresponding to insulators No 5 and 7, was found to be higher than the reference AR value indicating that these two insulators are aged with likely similar extent of degradation, in agreement with the LIBS diagnostic result (see Table 6 for the corresponding values of R, R_{Ref} and Table 5 for the corresponding values of AR). This is further confirmed by the fact that both insulators No 5 and No 7 have been characterized as semi-wettable. While the number of insulators tested is rather limited, the results, obtained, provide strong evidence for the validity and application of the proposed LIBS diagnostic procedure for assessing the type and quality of field-aged SIR insulators.

The next stage of the study involved implementation of the LIBS diagnostic procedure in the field. To this end, the remote LIBS system and diagnostic procedure for evaluating HV field-aged SIR insula-

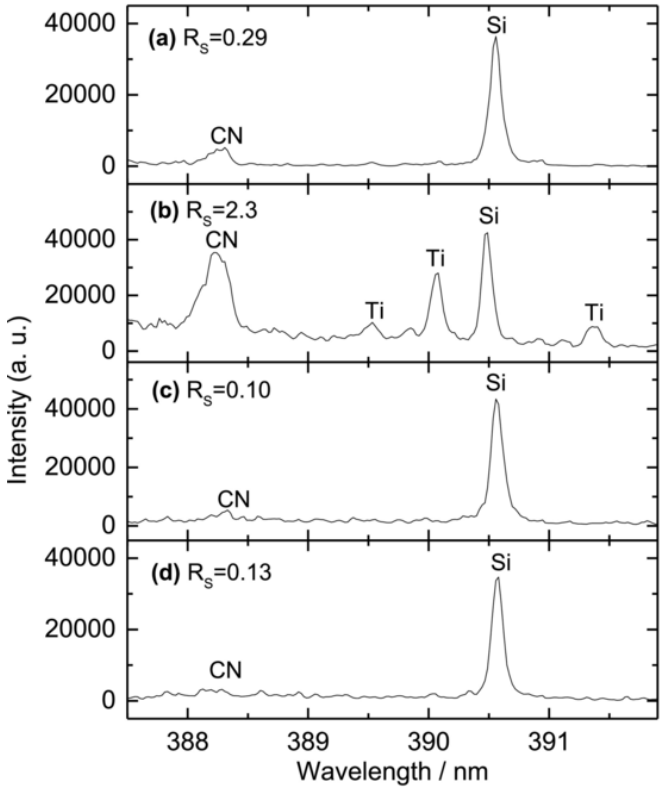

Fig. 8. Typical remote LIBS spectra of HV composite insulators recorded with the purpose to validate the suggested remote LIBS diagnostic procedure of field-aged SIR insulators. The spectra correspond to pristine SIR insulator (a) and field-aged insulators No 2 (b), No 5 (c) No 7 (d) and No 8 (e). The calculated surface spectral indicator (R_S) is noted in each case. Each spectrum represents an average of 10 single-laser-shot spectra, recorded upon irradiation of the surface of each insulator on a single spot (λ = 1064 nm; F_{LASER} = 10 J/cm^2; τ_D: 0.6 μs, τ_G: 1 μs).

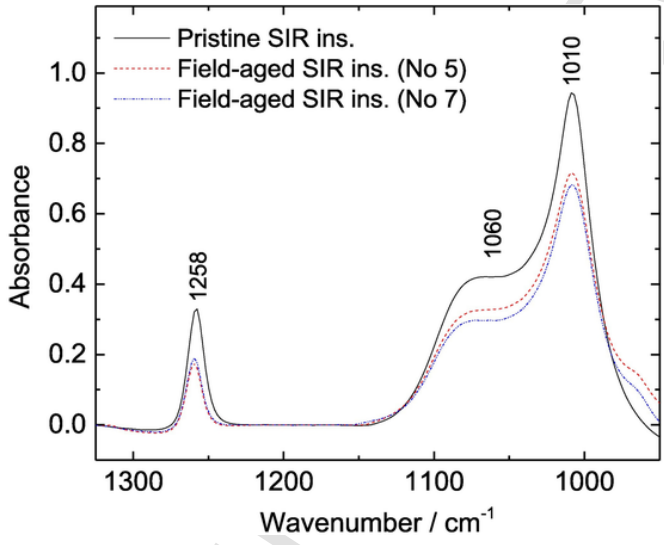

Fig. 9. ATR-FTIR spectra recorded on the surface of field-aged insulators No 5 and No 7, used for validation of the LIBS diagnostic procedure. A spectrum corresponding to a pristine SIR insulator is also plotted for comparison. The spectra are background corrected.

tors was tested at the Hellenic Electricity Distribution Network Operator (HEDNO) outdoor experimental facility (TALOS High Voltage Test Station) at Heraklion, where measurements were performed on a 10-year old HV outdoor field-aged insulator, which was available to be removed from the local network. A pristine SIR insulator was also measured, as reference, under the same conditions. The remote LIBS plasma collection system and typical spectra recorded onsite, are shown in Fig. 10. The spectral indicator value corresponding to the field-aged insulator was calculated to be lower than the reference value (R = 0.25 ± 0.03; R_{Ref} = 0.29 ± 0.03) and, according to the sorting criterion (C1), the insulator was classified as composed of SIR. Next, the spectral indicator for insulator physical condition was calculated to be %ΔR = (12 ± 13) % indicating that the insulator, tested, maintained its quality features. In addition, it was shown that the proposed LIBS methodology, which was tested and optimized in the laboratory, works quite well even outdoors, where factors such as sunshine, wind or dust affect measurements, causing signal fluctuations and significant reduction of the signal-to-noise ratio. In addition, ATR-FTIR spectroscopic measurements of samples, taken from the tested field-aged insulator, verified that its housing material is indeed SIR while the relevant absorbance bands were found to be weaker than the ones corresponding to a pristine SIR insulator. This information confirms the validity of LIBS measurements on-site and suggests that the proposed remote LIBS diagnostic procedure for determining the type and quality of field-aged SIR insulators is feasible to be performed in the field.

3.4. ATR-FTIR spectroscopic examination of laser irradiated areas of field-aged SIR insulators

An important aspect underlying the proposed methodology, which needs thorough investigation, relates to the unavoidable modification of the insulator surface during LIBS analysis. Laser ablation will result in some etching of the composite surface and a question arising is as to what extent this intense laser-composite interaction might affect the chemical structure of the polymer and bias the values of R. Several research groups [69,70] have reported that native PDMS films undergo chemical transformations upon ablation with laser pulses in the UV, Vis or IR. These modifications vary depending on the exposure parameters employed, for example, laser wavelength, pulse width and number of pulses. It is noted here that SIR, used in HV polymeric insulators, exhibits different optical and physicochemical properties compared to native PDMS films as a result of the application of high temperature vulcanization procedures and addition of fillers [33,71], therefore it is vulcanized silicone rubber that needs to be checked.

To this end, a series of ATR-FTIR spectroscopic measurements on several laser-irradiated areas of field-aged SIR insulators has been performed and the spectra were compared with the ones obtained from intact (non-irradiated) areas. In the remote LIBS mode, the laser affected spot, formed upon irradiation with 15 laser pulses, was almost equal in size with the spot probed by the ATR-FTIR spectrometer (0.03 cm^2). Fig. 11 shows typical ATR-FTIR spectra recorded from irradiated (15 laser pulses, F_{LASER} = 10 J/cm^2) and intact areas of a pristine (No 1) and a field-aged insulator (No 5) in the range 1300–650 cm^{-1}. For the pristine insulator, FTIR spectra from the irradiated areas are almost identical to those from intact areas. In the case of the field-aged insulator's spectra from irradiated areas show similar profile with those from non-irradiated areas but exhibit uniformly lower absorbance values. Based on the absorbance ratio values (AR) calculated from the spectra corresponding to the laser irradiated areas in comparison with the intact areas (on the surface) (see Table 7) we conclude that remote LIBS irradiation: a) results in negligible degradation in the case of a pristine insulator, since AR maintains a value similar to that before irradiation, b) causes small modifications in the case of field-aged insulators as reflected by AR values being slightly lower compared to the ones from intact areas. The subject of insulator surface modification during LIBS analysis requires additional studies possibly at microscopic resolution so as to reliably estimate to what extent laser ablation effects propagate into the calculation of the spectral indicator values.

Fig. 10. Remote LIBS demonstration at the Hellenic Electricity Distribution Network Operator (HEDNO) outdoor experimental facility (TALOS High Voltage Test Station in Heraklion) for the evaluation of HV outdoor insulators. (a) The insulator is removed from the power network and is placed on a special stage, designed to ensure nearly normal incidence of the laser beam on the insulator surface (b) Plasma emission is collected by a telescope, which is placed at approximately 10 m away from the target. An optical fiber is aligned at the focus of the telescope, transmitting the plasma light into the spectrometer. (c) Typical remote LIBS spectra of pristine and field-aged HV insulators. Each spectrum is an average of 10 successive single-shot spectra (λ = 1064 nm; F_{LASER} = 10 J/cm^2; τ_D: 1.28 μs, τ_G: 1 ms).

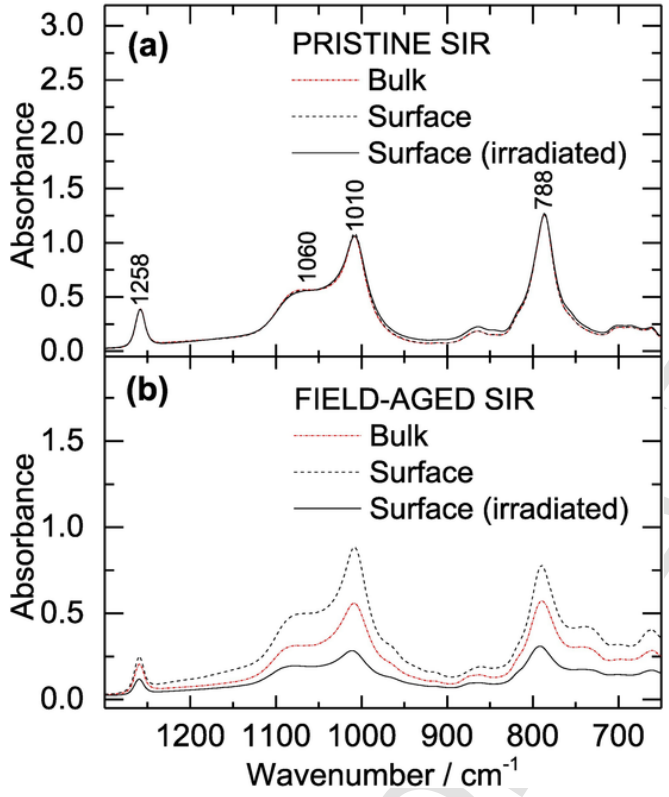

Fig. 11. ATR-FTIR spectra recorded from pristine insulator (a) and field-aged insulator No 5 (b) Three spectra are presented in each case, corresponding to the surface of non-irradiated areas (dash line), to the surface of laser irradiated areas (with 15 pulses at F_{LASER} = 10 J/cm^2, solid line) and to the bulk (short dash dot line) of the insulators.

Table 7
Absorbance ratio values (AR) calculated from ATR-FTIR spectra of field-aged SIR insulators comparing laser irradiated against intact areas.

Insulator no	Operation time (yrs)	AR [a] (Intact areas)	AR (Irradiated areas)
1	0	15 ± 1	15 ± 1
4	21	21 ± 1	19 ± 2
5	17	26 ± 1	18 ± 3
6	17	20 ± 2	18 ± 2
7	10	22 ± 1	20 ± 1

[a] AR = $I_{(1060–1010)}$/ I_{1258}. I: integrated intensity of the bands at 1060–1010 cm^{-1} and at 1258 cm^{-1} in the ATR-FTIR spectra corresponding to the surface of field-aged SIR insulators. The uncertainty in the calculation corresponds to the standard deviation in a set of 3–5 measurements.

4. Conclusions

In the present work, LIBS was used for the analysis of several field-aged HV insulators and was found to be a promising field-deployable technique for performing efficient and reliable assessment of the physical state of HV outdoor insulators in service. Remote (on-site) LIBS was demonstrated (as a proof of principle) to be a fast, reliable and effective method for the evaluation of the physical condition of HV outdoor SIR insulators. A stand-off LIBS diagnostic procedure was based on the use of specific LIBS spectral indicators (R and ΔR) of the type and quality of SIR insulators and resulted in the formulation of sorting and evaluation criteria.

The sorting criterion (C1) is based on LIBS spectral indicator R, which reflects the concentration ratio of the main chemical constituents (C and Si) of the insulators polymeric housing. Indicator R is defined as the ratio of the integrated CN band head molecular emission intensity over the integrated Si atomic emission intensity (CN: 388.34 nm; Si I: 390.55 nm) and serves as a quick probe determining the type of the field-aged insulator (SIR or not SIR). The value of R permits screening between SIR and non-SIR insulators with $R < 0.3$ suggesting the presence of SIR. The validity of this sorting criterion is confirmed by ATR-FTIR measurements. Concerning the ageing of SIR insulators, the value of the relative difference indicator (%ΔR) represents the deviation of the R value, measured on the surface of a field-aged insulator, from that corresponding to a pristine one and reflects the extent of surface degradation. It is suggested that in cases for which ΔR > 30% the examined insulators are of moderate or low quality (criterion C3).

Future work will focus on the optimization of the proposed remote LIBS diagnostic procedure by using high energy output lasers and targeting the insulators through a telescope with the aim to extend analysis at longer distances the ultimate goal being the development of a transportable, robust system capable to operate outdoors and at rough terrains. Furthermore, automation of the diagnostic procedure that might involve the use of data processing tools and chemometrics [72–74] and would end up in an integrated tool, useable by non-experts, is necessary. Undoubtedly, such improvements are a prerequisite for achieving fast, convenient and effective real time monitoring of the physical condition of in-service HV composite insulators, towards the goal of maintaining highly efficient and reliable power transmission networks.

Uncited references

[21,66]

Declaration of Competing Interest

The authors declare that they have no known competing financial interests or personal relationships that could have appeared to influence the work reported in this paper.

Acknowledgements

This work was supported by the POLYDIAGNO research project (11ΣΥΝ-7-1503), implemented in the framework of the Operational Program "Competiveness and Entrepreneurship", Action "Cooperation 2011", co-financed by the European Union (European Regional Development Fund) and Greek national funds (National Strategic Reference Framework 2007-2013). The authors would like to thank G. Kenanakis for providing access to the ATR-FTIR spectrometer and P. Siozos for his valuable help in remote LIBS measurements performed at the TALOS High Voltage Test Station.

References

[1] J. Kim, M.K. Chaudhury, M.J. Owen, Hydrophobicity loss and recovery of silicone HV insulation, IEEE Trans. Dielectr. Electr. Ins. 6 (1999) 695–702.
[2] H. Hillborg, U.W. Gedde, Hydrophobicity recovery of polydimethysiloxane after exposure to corona discharges, Polymer 39 (1998) 1991–1998.
[3] H. Hillborg, U.W. Gedde, Hydrophobicity changes in silicone rubbers, IEEE Trans. Dielectr. Electr. Ins. 6 (1999) 703–717.
[4] D. Ghosh, D. Khastgir, Degradation and stability of polymeric HV insulators and prediction of their service life through environmental and accelerated aging processes, ACS Omega 3 (2018) 11317–11330.
[5] T. Sorqvist, S.M. Gubanski, Leakage current and flashover of field-aged polymeric insulators, IEEE Trans. Dielectr. Electr. Ins. 6 (1999) 744–753.
[6] P.D. Blackmore, D. Birtwhistle, G.A. Cash, G.A. George, Condition assessment of EPDM composite insulators using FTIR spectroscopy, IEEE Trans. Dielectr. Electr. Ins. 5 (1998) 132–141.
[7] A. Toth, I. Bertoti, M. Blazso, G. Banhegyi, A. Bognar, P.J. Szaplonczay, Oxidative damage and recovery of silicone-rubber surfaces. 1. X-ray photoelectron spectroscopic study, J. Appl. Polym. Sci. 52 (1994) 1293–1307.
[8] S. Hunt, G. Cash, H. Liu, G. George, D.J. Birtwistle, Spectroscopic characterization of low molecular weight fluids from silicone elastomers, Macromol. Sci. A 39 (2002) 1007–1024.
[9] H. Liu, G. Cash, D. Birtwhistle, G. George, Characterization of a severely degraded silicone elastomer HV insulator. An aid to development of lifetime assessment techniques, IEEE Trans. Dielectr. Electr. Ins. 12 (2005) 478–486.
[10] V. Rajini, K. Udayakumar, Degradation of silicone rubber under AC or DC voltages in radiation environment, IEEE Trans. Diel. Electr. Ins. 16 (2009) 834–841.
[11] A. Tzimas, E. Da Silva, S.M. Rowland, B. Boumecid, M. Queen, M. Michel, Asset management frameworks for outdoor composite insulators, IEEE Trans. Dielectr. Ins. 19 (2012) 2044–2054.
[12] S.M. Gubanski, A. Dernfalk, J. Andersoon, H. Hillborg, Characterization of a severely degraded silicone elastomer HV insulator. An aid to development of lifetime assessment techniques, IEEE Trans. Dielectr. Electr. Ins. 14 (2007) 1065–1080.
[13] F. Schmuck, J. Seifert, I. Gutman, A. Pigini, Assessment of the Condition of Overhead Line Composite Insulators CIGRE B2-214, 2012, pp. 1–10.
[14] L.E. Lundgaard, W. Hansen, Acoustic method for quality control and in-service periodic monitoring of medium voltage cable terminations, Proc. 1998 IEEE Int. Symp, 1, On Electrical Insulation Arlington, VA, USA, 1998, pp. 130–133.
[15] I. Urbaniec, P. Fracz, Application of UV camera for PD detection on long rod HV insulator, Meas. Autom. Monitoring 61 (2015) 64–67.
[16] A. Larsson, S. Kröll, A.D. Dernfalk, S.M. Gubanski, In-situ diagnostics of high-voltage insulation using laser-induced fluorescence spectroscopy, IEEE Trans. Dielectr. Electr. Insul. 9 (2002) 274–281.
[17] S. Wallström, A.D. Dernfalk, M. Bengtsson, S. Kröll, S.M. Gubanski, S. Karlsson, Image analysis and laser induced fluorescence combined to determine biological growth on silicone rubber insulators, Polym. Degrad. Stab. 88 (2005) 394–400.
[18] A.S. Vaughan, S.J. Dodd, S.J. Sutton, A Raman microprobe study of electrical treeing in polyethylene, J. Mater. Sci. 39 (2004) 181–191.
[19] A.S. Vaughan, I.L. Hosier, S.J. Dodd, S.J. Sutton, On the structure and chemistry of electrical trees in polyethylene, J. Phys. D. Appl. Phys. 39 (2006) 962–978.
[20] O. Kokkinaki, A. Klini, D. Anglos, N. Mavrikakis, E. Koudoumas, K. Siderakis 2019 (unpublished results).
[21] R. Srinivasan, UV laser ablation of polymers, in: L.D. Laude, D. Bäuerle, M. Wautelet (Eds.), Interfaces Under Laser Irradiation, 134, Springer, Netherlands, 1987, pp. 359–370.
[22] B. Pinnangudi, R.S. Gorur, C.D. Poweleit, Quantification of degradation in nonceramic insulator housing materials by laser ablation, IEEE Trans. Diel. Electr. Ins. 13 (2006) 423–429.
[23] I.L. Hosier, M.S. Abd Rahman, A.S. Vaugha, A. Krivda, X. Kornmann, L.E. Schmidt, Comparison of laser ablation and inclined plane tracking tests as a means to rank materials for outdoor HV insulators, IEEE Trans. Dielectr. Electr. Insul. 20 (2013) 1808–1819.
[24] S. Palanco, J. Laserna, Remote sensing instrument for solid samples based on open-path atomic emission spectrometry, Rev. Sci. Instrum. 75 (2004) 2068–2074.
[25] F.J. Fortes, J.J. Laserna, The development of fieldable laser-induced breakdown spectrometer: no limits on the horizon, Spectrochim. Acta B 65 (2010) 975–990.
[26] M.M. Tripathi, K.E. Eseller, F.Y. Yueh, J.P. Singh, An optical sensor for multi-species impurity monitoring in hydrogen fuel, Sensors Actuators B 171–172 (2012) 416–422.
[27] R.S. Harmon, R.E. Russo, R.R. Hark, Applications of laser-induced breakdown spectroscopy for geochemical and environmental analysis: a comprehensive review, Spectrochim. Acta B 87 (2013) 11–26.
[28] R. Noll, C. Fricke-Begermann, S. Connemann, C. Meinhardt, V. Sturm, LIBS analyses for industrial applications – an overview of developments from 2014 to 2018, J. Anal. Atom. Spectrom. 33 (2018) 945–956.
[29] V.K. Singh, J. Sharma, A.K. Pathak, C.T. Ghany, M.A. Gondal, Laser-induced breakdown spectroscopy (LIBS): a novel technology for identifying microbes causing infectious diseases, Biophys. Rev. 10 (2018) 1221–1239.
[30] M. Bengtsson, R. Gronlund, M. Lundqvist, A. Larsson, S. Kroll, S. Svanberg, Remote laser-induced breakdown spectroscopy for the detection and removal of salt on metal and polymeric surfaces, Appl. Spectrosc. 60 (2006) 1188–1191.
[31] X. Wang, X. Hong, P. Chen, C. Zhao, Z. Jia, L. Wang, L. Zou, Surface hardness analysis of aged composite insulators via laser-induced plasma spectra characterization, IEEE Trans Plasma Sci. 47 (2019) 387–394.
[32] P. Chen, X. Wang, X. Li, Q. Lyu, N. Wang, Z. Jia, A. Quick Classifying, Method for tracking and erosion resistance of HTV silicone rubber material via laser-induced breakdown spectroscopy, Sensors 19 (2019) 1–15 1087.
[33] K. Papailiou, F. Schmuck, Silicone Composite Insulators, Springer-Verlag, Berlin Heidelberg, 2013.
[34] M. Dimitropoulou, D. Pylarinos, K. Siderakis, E. Thalassinakis, M. Danikas, Insulation coordination and pollution measurements in the island of Crete, ICPADM International Conference on the Properties and Applications of Dielectric Materials, 2015 Sydney, Australia, July 19-22.
[35] D.A. Cremers, L.J. Radziemski, Handbook of Breakdown Spectroscopy, John Wiley & Sons, Ltd, England, 2006, pp. 171–196 Chap. 7.
[36] D. Pylarinos, K. Siderakis, E. Thalassinakis, N. Mavrikakis, A new approach for open air insulator test stations: experience from talos and the polydiagno project, J. Electr. Eng. 16 (2016) 269–273.
[37] G. Momen, M. Farzaneh, Survey of micro/nano filler use to improve silicone rubber for outdoor insulators, Rev. Adv. Mater. Sci. 27 (2011) 1–13.
[38] A. Theodoridis, M.G. Danikas, J. Soulis, Room temperature vulcanized (RTV) silicone rubber coatings on glass and porcelain insulators: an effort to model their behaviour under contaminated conditions, J. Electr. Eng. 52 (2001) 63–67.
[39] L. St-Onge, R. Sing, S. Béchard, M. Sabsabi, Carbon emissions following 1.064 μm laser ablation of graphite and organic samples in ambient air, Appl. Phys. A Mater. Sci. Process. 69 (1999) S913–S916.
[40] S. Grégoire, M. Boudinet, F. Pelascini, F. Surma, V. Detalle, Y. Holl, Laser-induced breakdown spectroscopy for polymer identification, Anal. Bioanal. Chem. 400 (2011) 3331–3340.
[41] S. Trautner, J. Jasik, C.G. Parigger, J.D. Pedarnig, W. Spendelhofer, J. Lackner, P. Veis, J. Heitz, Laser-induced optical breakdown spectroscopy of polymer materials based on evaluation of molecular emission bands, Spectrochim. Acta B 174 (2017) 331–338.
[42] T. Sorqvist, A.E. Vlastos, Performance and ageing of polymeric insulators, IEEE Trans. Power Deliv. 12 (1997) 1657–1665.
[43] J. Morvan, M. Camelot, P. Zecchini, C.J. Roques-Carmes, Infrared investigation of the role of ozone oxidation in the adhesion of polydimethylsiloxane films, Colloid Interface Sci. 97 (1984) 149–156.
[44] G. Socrates, Infrared and Raman characteristic group frequencies-Tables and Charts, 3rd ed, John Wiley & Sons; Ltd, England, 2001 Copyright.
[45] D. Cai, A. Neyer, R. Kuckuk, H.M. Heise, Raman, mid-infrared and ultraviolet-visible spectroscopy of PDMS silicone rubber for characterization of polymer optical wavegude materials, J. Mol. Struct. 976 (2010) 274–281.
[46] S. Mitra, A. Ghanbari-Siahkali, P. Kingshott, S. Hvilsted, K. Almdal, An investigation on changes in chemical properties of pure ethylene-propylene-diene rubber in aqueous acidic environments, Mater. Chem. Phys. 98 (2006) 248–255.
[47] P. Mani, S. Suresh, Vibrational spectra and normal coordinate analysis of acetic acid cyclohexyl ester, Rasayan J. Chem 2 (2009) 307–311.
[48] L.D. Frederickson, Characterization of hydrated aluminas by infrared spectroscopy, Anal. Chem. 26 (1954) 1883–1885.
[49] R.L. Hubbard, K.E. Stanfield, W.C. Kommes, Anhydrous alumina as absorbent in constituent analysis of asphalt, Anal. Chem. 24 (1952) 1490–1491.
[50] H.A. Al-Abadleh, V.H. Grassian, FT-IR study of water adsorption on aluminum oxide surfaces, Langmuir 19 (2003) 341–347.
[51] C.A. Ríos Reyes, C. Williams, O.M. Castellanos Alarcón, Nucleation and growth process of sodalite and cancrinite from kaolinite-rich clay under low-temperature hydrothermal conditions, Mater. Res. 16 (2013) 424–438.
[52] P.D. Blackmore, D. Birtwhistle, G.A. Cash, G.A. George, Condition assessment of EPDM composite insulators using FTIR spectroscopy, IEEE Trans. Dielelectr. Electr. Ins. 5 (1998) 132–141.
[53] E. San Andrés, A. del Prado, F.L. Martínez, I. Mártil, D. Bravo, F.J. López, Rapid thermal annealing effects on the structural properties and density of defects in SiO_2 and SiN_x: H films deposited by electron cyclotron resonance, J. Appl. Phys. 87 (2000) 1187–1192.
[54] B.J. Saikia, G. Parthasarathy, Fourier transform infrared spectroscopic characterization of kaolinite from Assam and Meghalaya, Northeastern India, J. Mod. Phys. 1 (2010) 206–210.

[55] P.G. Pai, S.S. Chao, Y. Takagi, G. Lucovsky, Infrared spectroscopic study of SiOx films produced by plasma enhanced chemical vapor deposition, J. Vac. Sci. Tech. A 4 (1986) 689–694.
[56] S. Kumagai, X. Wang, N. Yoshimura, Solid residue formation of RTV silicone rubber due to dry-band arcing and thermal decomposition, IEEE Trans. Dielectr. Electr. Ins. 5 (1998) 281–289.
[57] E.A. Cherney, Silicone rubber dielectrics modified by inorganic fillers for outdoor high voltage insulation applications, IEEE Trans. Dielectr. Electr. Ins. 12 (2005) 1108–1115.
[58] H. Khan, M. Amin, A. Ahmad, M. Yasin, Impact of alumina trihydrate and silica on mechanical, thermal and electrical properties of silicone rubber composites for high voltage insulations, Res. Dev. Mater. Sci. 2 (2017) 153–160.
[59] N. Mavrikakis, K. Siderakis, E. Koudoumas, E. Drakakis, E. Kymakis, Laboratory investigation of the hydrophobicity transfer mechanism on composite insulators aged in coastal service, Eng. Tech. App. Sci. Res. 6 (2016) 1124–1129.
[60] A. Hergert, J. Kindersberger, C. Bär, R. Bärsch, Transfer of hydrophobicity of polymeric insulating materials for HV outdoor application, IEEE Trans. Diel. Electr. Engin. 24 (2017) 1057–1067.
[61] A.E. Vlastos, S.M. Gubanski, Surface structural changes of naturally aged silicone and EPDM composite insulators, IEEE Trans. Power Deliv. 6 (1991) 888–896.
[62] N.C. Mavrikakis, P.N. Mikropoulos, K. Siderakis, Evaluation of field-ageing effects on insulating materials of composite suspension insulators, IEEE Trans. Dielectr. Electr. Insul. 24 (2017) 490–498.
[63] H. Cao, D. Yan, J. Han, H. Ren, M. Lu, Z. Lv, H. Guo, Investigation and corroboration of a novel method to estimate the hydrophobicity of composite insulators, IEEE Trans. Dielectr. Electr. Insul. 19 (2012) 2029–2036.
[64] IEC TS 62073, Technical specification, Guidance on the Measurement Of Wettabilty of Insulator Surfaces, First edition, 2003–06.
[65] N. Mavrikakis, K. Siderakis, P.N. Mikropoulos, Laboratory Investigation On Hydrophobicity and Tracking Performance Of Field Aged Composite Insulators, UPEC, 2014 conference, doi:10.1109/UPEC.2014. 6934665.
[66] H. Cao, D. Yan, J. Han, H. Ren, M. Lu, Z. Lv, H. Guo, Investigation and corroboration of a novel method to estimate the hydrophobicity of composite insulators, IEEE Trans. Dielectr. Electr. Insul. 19 (2012) 2029–2036.
[67] S. Guirado, F.J. Fortes, J.J. Laserna, Elemental analysis of materials in an underwater archaeological shipwreck using a novel remote laser-induced breakdown spectroscopy system, Talanta 137 (2015) 182–188.
[68] F. Marinello, A. Pezzuolo, A. Chiumenti, L. Sartori, Technical analysis of unmanned aerial vehicles (drones) for agricultural applications, Eng. Rural Dev. 25–27 (2016) 870–875 Jelgava, Latvia May.
[69] N.E. Stankova, P.A. Atanasov, R. Nikov, R.G. Nikov, N.N. Nedyalkov, T.R. Stoyanchov, N. Fukata, K.N. Kolev, E. Valova, J.S. Georgieva, S. Armyanov, Optical properties of polydimethylsiloxane (PDMS) during nanosecond laser processing, Appl. Surf. Sci. 374 (2016) 96–103.
[70] V.-M. Graubner, R. Jordan, O. Nuyken, T. Lippert, A. Wokaun, S. Lazare, L. Servant, Local chemical transformations in poly(dimethylsiloxane) by irradiation with 248 nm and 266 nm, Appl. Surf. Sci. 197 (2002) 786–790.
[71] R. Hackam, Outdoor HV composite polymeric insulators, IEEE Trans. Dielectr. Electr. Insul. 6 (1999) 557–585.
[72] R. Sattmann, I. Mönch, H. Krause, R. Noll, S. Couris, A. Hatziapostolou, A. Mavromanolakis, C. Fotakis, E. Larrauri, R. Miguel, Laser-induced spectroscopy for polymer identification, Appl. Spectrosc. 52 (1998) 456–461.
[73] M. Boueri, V. Motto-Ros, W.-Q. Lei, Q.-L. Ma, L.-J. Zheng, H.-P. Zeng, J. Yu, Identification of polymer materials using laser-induced breakdown spectroscopy combined with artificial neural networks, Appl. Spectrosc. 65 (2011) 307–314.
[74] J.J. Laserna, Advanced recognition of explosives in traces on polymer surface supervised LIBS and supervised learning classifiers, Anal. Chim. Acta 806 (2014) 107–116.